Overexpression of the key metabolic protein CPT1A defines mantle cell lymphoma patients with poor response to standard high-dose chemotherapy independent of MIPI and complement established high-risk factors

Anna Sandström Gerdtsson,[1] Joana de Matos Rodrigues,[1] Christian Winther Eskelund,[2] Simon Husby,[2] Kirsten Grønbæk,[2] Riikka Räty,[3] Arne Kolstad,[4] Christian Geisler,[2] Anna Porwit,[5] Mats Jerkeman[6] and Sara Ek[1]

[1]Department of Immunotechnology, Lund University, Lund, Sweden; [2]Department of Hematology, Rigshospitalet, Copenhagen, Denmark; [3]Department of Hematology, Helsinki University Hospital, Helsinki, Finland; [4]Department of Oncology, Oslo University Hospital, Oslo, Norway; [5]Department of Clinical Sciences, Oncology and Pathology, Lund University, Lund, Sweden and [6]Department of Oncology, Lund University Hospital, Lund, Sweden

Correspondence: S. EK
sara.ek@immun.lth.se

Received: May 24, 2022.
Accepted: November 28, 2022.
Early view: December 15, 2022.

https://doi.org/10.3324/haematol.2022.281420

Abstract

The variable outcome to standard immunochemotherapy for mantle cell lymphoma (MCL) patients is a clinical challenge. Established risk factors, including high MCL International Prognostic Index (MIPI), high proliferation (Ki-67), non-classic (blastoid/pleomorphic) morphology, and mutated *TP53*, only partly identify patients in need of alternative treatment. Deepened understanding of biological factors that influence time to progression and relapse would allow for an improved stratification, and identification of novel targets for high-risk patients. We performed gene expression analyses to identify pathways and genes associated with outcome in a cohort of homogeneously treated patients. In addition to deregulated proliferation, we show that thermogenesis, fatty acid degradation and oxidative phosphorylation are altered in patients with poor survival, and that high expression of carnitine palmitoyltransferase 1A (CPT1A), an enzyme involved in fatty acid degradation, can specifically identify high-risk patients independent of the established high-risk factors. We suggest that complementary investigations of metabolism may increase the accuracy of patient stratification and that immunohistochemistry-based assessment of CPT1A can contribute to defining high-risk MCL.

Introduction

Mantle cell lymphoma (MCL) is a mature B-cell lymphoma with heterogeneous presentation and aggressive evolution upon progression.[1] The primary pathogenic event is marked by the genetic translocation t(11;14)(q13,q32), which results in upregulation of *CCND1* with constitutive overexpression of Cyclin D1 and deregulation of the cell cycle at the S1-G transition.[2] Albeit essential for MCL development, Cyclin D1 has a limited oncogenic effect and secondary mechanisms are required to drive full malignant transformation. Genomic investigations have identified several genetic alterations, including *ATM, TP53, BIRC3, NOTCH1, CCND1, KMT2D*.[3,4] The genomic landscape of MCL is heterogeneous, which complicates the design of novel treatment strategies. In a recent study, we showed that only 21% of tumors harbored actionable mutations.[4]

The age and fitness of the patient are still the main factors for selecting frontline therapy, with young (≤65 years) and fit patients receiving chemoimmunotherapy, including high-dose cytarabine, rituximab and autologous stem cell transplantation (ASCT). However, response to treatment is variable, and more tailored regimens and companion biomarkers are required for improved survival of high-risk patients. Current clinical trials focus on the use of combinations of BTK inhibitors,[5] CD20 antibodies, venetoclax and/or chimeric antigen receptor T-cell (CAR T) therapy

for high-risk or refractory patients.[6] Therapeutic strategies complementary to these would enhance the possibilities to further adapt treatment both at diagnosis and in the relapsed setting based on the biological activity of the tumor.

The MCL International Prognostic Index (MIPI), is useful for prognostication but is currently not in clinical use to stratify patients. The known biological risk factors of MCL are frequently overlapping and include proliferation index assessed by Ki-67 staining, blastoid/pleomorphic (from here referred to as non-classic) morphology and *TP53* mutations. It has been proposed that a combined strategy of assessing MIPI, proliferation and *TP53* mutational status[7] would allow clinicians to keep low-risk patients on standard treatment while identifying high-risk patients in need of alternative, possibly chemotherapy-free regimens. However, among low-risk patients, the response to standard high-dose chemotherapy is variable, indicating that additionally unknown biological factors contribute to a short time to progression (TTP).

The main aim of this study was to identify complementary strategies to find patients with low probability to respond to intensive chemoimmunotherapy, and to determine potential novel targets that are relevant for those patients. We found that thermogenesis, fatty acid degradation and oxidative phosphorylation are deregulated in patients with poor response to the Nordic MCL 2 and 3 (N-MCL2/3) clinical trials protocol which includes high-dose cytarabine. In particular, the overexpression of carnitine palmitoyltransferase 1A (CPT1A), a key factor for lipid metabolism, was validated on the protein level as negatively associated with TTP and overall survival (OS), both as a continuous and dichotomized variable. CPT1A overexpression was shown to be independent of established risk factors, such as proliferation and morphology. The association between CPT1A and OS was validated in an independent population-based patient cohort. We suggest that an improved risk stratification of MCL patients can be achieved through assessment of CPT1A at diagnosis.

Methods

Patient samples

Samples for gene expression (GEX) (n=70) and immunohistochemistry (IHC) (n=45) analysis were selected from the N-MCL2/3 clinical trial cohort (*clinicaltrials gov. Identifiers: NCT00514475* and *ISRCTN87866680*).[8,9] Samples had been previously collected from 2000 to 2006 (N-MCL2) and from 2005 to 2009 (N-MCL3), and patients had been treated with first-line R-CHOP (rituximab, cyclophosphamide, doxorubicin vincristine, and prednisone), high-dose cytarabine cycles and ASCT. Mutational status of *ATM* and *TP53* had been previously collected using custom design multiplex Ion Ampliseq.[10] A population-based MCL cohort (n=135) from the biobank of lymphomas in Southern Sweden (BLISS) including patients diagnosed from 2000 to 2014, was used to validate the expression of individual proteins. The studies were approved by the Ethical Review Boards in Lund (Dnr 2011/593, BLISS; Dnr 2006/242, N-MCL2/3) and Uppsala (Dnr 2009/428, N-MCL2/3). An overview of the cohort used is shown in Figure 1.

Transcriptome analysis

RNA was isolated using the RecoverAll total nucleic acid isolation kit (Ambion, Carlsbad, CA). RNA quantity (optical density [OD] 260 nm) and quality (260 nm/280 nm) were assessed using ND-1000 spectrophotometry (Thermo Scientific, Wilmington, DE). GEX was measured using GeneChip Human Gene ST 1.0 whole transcript arrays (Applied Biosystems, MA, USA), measuring >25 probes per transcript. R (version 4.1.1) and R studio (version 2021.09.0) were used for data analysis. The maEndtoEnd workflow (version 3.13)[11] was used to identify differentially expressed genes (DEG) for *TP53*-mutated *versus* wild-type (wt), Ki-67 high *versus* low, non-classic *versus* classic morphology, *ATM*-mutated *versus* wt, excluding *TP53*-mutated samples (n=10) from all but the first comparison. Survival-associated genes were identified by fitting a Cox regression model independently for each gene. PathfindR (version 1.6.2)[12] was used for pathway analysis based on KEGG gene lists, Biogrid protein-protein interaction networks, and the number of iterations set to 5, with the following gene lists input criteria: log rank<0.01 (survival); P<0.05 (*TP53* status); P<0.001 (morphology); P<0.0001 (proliferation).

Protein analysis

Tissue microarray blocks were assembled as previously described.[13] For IHC, slides were pretreated using the DAKO PT link system (DAKO; Glostrup, Copenhagen, Denmark) and stained in an Autostainer Plus (DAKO; Glostrup, Copenhagen, Denmark) with the following antibodies: anti-FEN1 (1:1,500, ab109132 Abcam, Cambridge, UK), anti-CPT1A (1:1,800, ab128568, Abcam, Cambridge, UK) and anti-WEE1 (1:200, sc-5285, Santa Cruz, Texas, USA). Slides were scanned at X20 magnification using a NanoZoomer 60 (Hamamatsu Photonics, Shizuoka, Japan) and evaluated with HALO® (Indica Labs, New Mexico, USA). Cox proportional hazard (PH) models were used to estimate the hazard ratio (HR) for CPT1A, FEN and WEE1, using date of diagnosis/treatment start as starting point, and date of death of any cause (BLISS and N-MCL2/3) and date of documented relapse or progression (N-MCL2/3) as endpoints for OS and TTP, respectively. The PH assumption was tested using the Therneau and Grambsch test of the Schoenfeld residuals. Maxstat[14] was used to define cut-offs, log-rank statistics to evaluate differences between

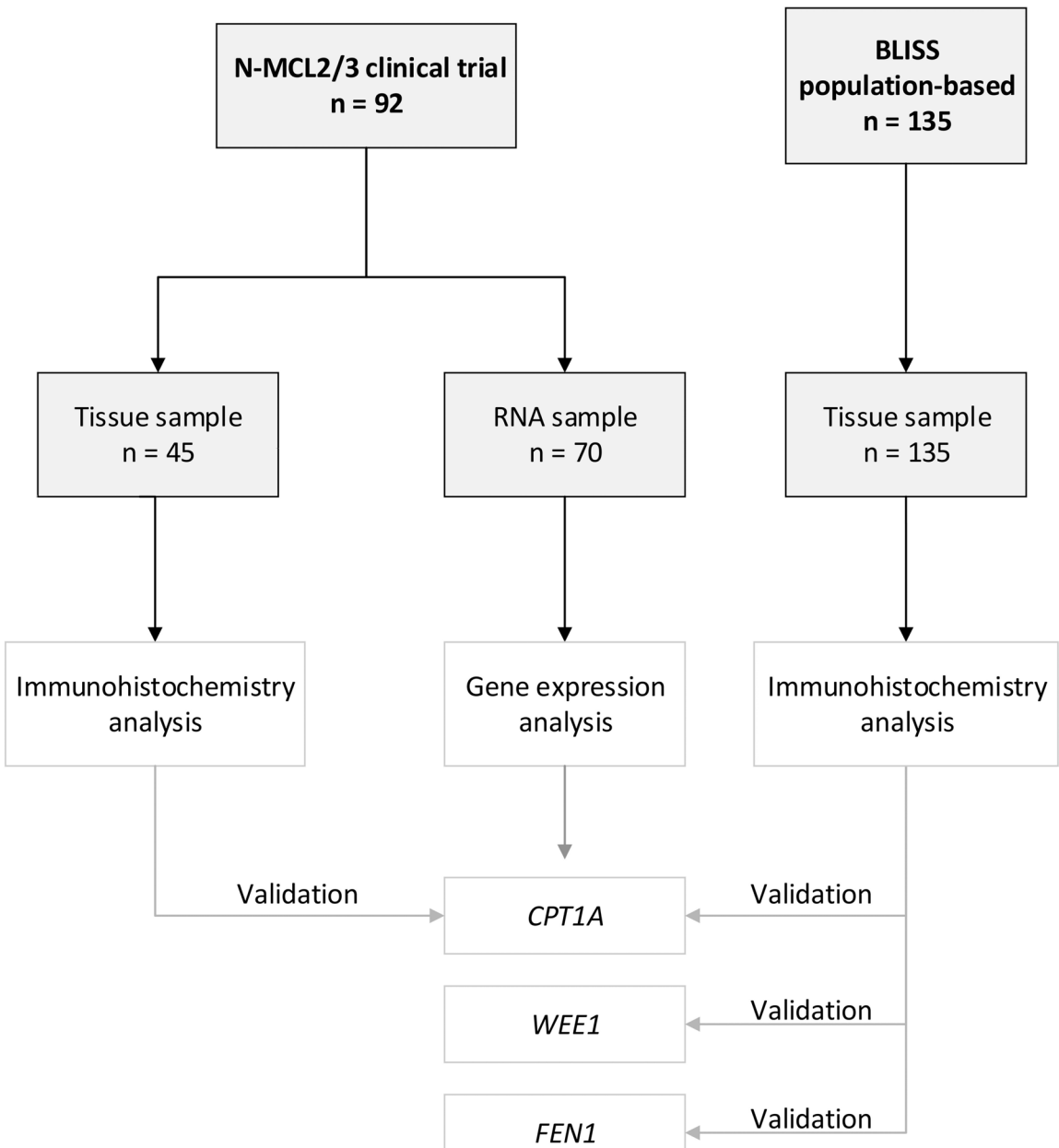

Figure 1. A flow diagram summarizing the cohorts used. RNA samples from the Nordic MCL2 and MCL3 trials were used for gene expression analyses. Partly overlapping samples from the same clinical trial material was available for validation of corresponding proteins. An independent population-based cohort, biobank of lymphomas in Southern Sweden (BLISS), was used to validate CPT1A, WEE1 and FEN1 protein expression.

survival curves, and Wilcoxon signed-rank test to compare differences between groups.

Results

Cohorts used for exploration and validation

Diagnostic biopsies (n=70) from the N-MCL2/3 clinical trials were used for whole-transcript expression analysis to identify genes and pathways associated with poor outcome (TTP and OS, respectively) and established risk factors (Table 1). Biopsies available as TMA from N-MCL2/3 (n=45) and BLISS (n=135) were used to validate expression of individual proteins, using IHC followed by digital scoring. The N-MCL2/3 inclusion criteria were age ≤65 years, Ann-Arbor stage II-IV and no previous cancer treatment. Patients were homogeneously treated, including immunochemotherapy. In contrast, the population-based BLISS cohort included MCL patients treated with different therapies, the most frequent being R-Bendamustine. Information on Ki-67, morphology, *TP53* mutation status,[10] p53 immunoreactivity[15] was available for most samples. For Ki-67 and p53, a 30% cut-off was used to define high and low proliferation and/or p53. MIPI was available for most patients included in the N-MCL2/3 but only for a minority of patients in the population-based BLISS cohort. Patients were divided into MIPI low, intermediate, and high, according to the established scoring system.[16] The majority (67-77%) of patients were male, reflecting the male dominance of MCL prevalence. Due to differences in inclusion criteria and treatments, N-MCL2/3 patients had lower risk (62% MIPI low) than BLISS (44% MIPI high). The median OS in the BLISS cohort was only 4.2 years, compared to 11 and 12.4 years in the N-MCL2/3 GEX and IHC cohorts, respectively. The discovery cohort had been selected from the N-MCL2/3 material to represent a wide survival range and to reflect variable MCL risk factors. The samples used for GEX analysis thus had higher frequencies of non-classic morphology and high proliferation cases, compared to the full N-MCL2/3 cohort (n=319)[8-10]. While OS was similar to the full N-MCL2/3 cohort (11 years *vs*. 12.5 years), TTP was shorter in the selected cohort (5.3 years *vs.* 8.2 years).

Pathways of poor prognosis in mantle cell lymphoma

Genes associated with inferior TTP and OS were identified using Cox regression. Upregulated cell cycle (P=6.6x10^{-11})

Table 1. Clinicopathological characteristics of the different cohorts used in this study.

	N-MCL2/3 (mRNA)	N-MCL2/3 (IHC)	BLISS (IHC)
Overall, N	70	45	135
Sex, N (%) Male Female	 51 (73) 19 (27)	 30 (67) 15 (33)	 104 (77) 31 (23)
Age in years at diagnosis, median (min-max)	55 (37-65)		
MIPI, N (%) Low risk Medium risk High risk Missing	 34 (49) 17 (24) 19 (27)	 28 (62) 10 (22) 7 (16)	 11 (18) 24 (38) 27 (44) 73
Morphology, N (%) Classic Blastoid/pleomorphic Missing	 51 (73) 19 (27)	 39 (87) 6 (13)	 116 (91) 12 (9) 7
KI-67, N (%) <30% >30% Missing	 42 (60) 28 (48)	 28 (68) 13 (32) 4	 106 (80) 27 (20) 2
TP53, N (%) Wild-type Mutated Missing	 35 (78) 10 (22) 25	 22 (82) 5 (19) 18	 48 (77)) 14 (23) 73
Overall survival time in years, median	11	12.4	4.2
Time to progression in years, median	5.3	10	

Percentages might not add to 100% due to rounding. IHC: immunohistochemistry; MIPI: mantle cell lymphoma International Prognostic Index; N-MCL2/3: Nordic MCL group clinical trials 2 and 3. Corresponding values for the full (n=319) N-MCL2/3 cohort have been reported previously.[8-10]

and related pathways were dominating among genes associated with short TTP, followed by DNA repair pathways, thermogenesis and fatty acid degradation (Figure 2A-C). Inferior OS was primarily associated with oxidative phosphorylation (P=6.8x10^{-08}) and related pathways (Figure 3A-C). Proliferation has repeatedly been demonstrated to be associated to poor MCL prognosis and adding proliferation to the MIPI score has been shown to improve the prognostic value.[17-19] Concordantly, we identified strong upregulation of cell cycle-regulating genes including *CCNE1, CDC45, CDC25C, WEE1, TTK, MAD2L2, CDC25A, SKP, CHEK2*, and *MCM4* in shorter TTP and/or OS. However, targeting proliferation by cytostatic drugs has proven insufficient to cure MCL, indicating that other mechanisms are in place and should be identified.

Mitochondrial fatty acid transportation and metabolism are associated with inferior survival

Investigations beyond cell cycle and DNA repair mechanisms identified upregulation of metabolic pathways of thermogenesis, oxidative phosphorylation and fatty acid degradation as significantly associated with shorter TTP and OS. Upregulated genes were involved in fatty acid transportation into mitochondria, fatty acid degradation, and mitochondrial respiration, including *CPT1A, SLC25A20, ACAA1, ACAA2, NADH dehydrogenases, Cytochrome c oxidases*, and *PPA1*. Of interest, *CPT1A* and *SLC25A20* (CACT) are involved in the carnitine shuttle and import of long-chain fatty acids across the outer and inner mitochondrial membrane, respectively, while *ACAA2* catalyses the last step of the mitochondrial fatty acid β-oxidation (Figure 4A). Upregulation of transcripts involved in the downstream mitochondrial respiratory chain, including *NDUFB9, NDUFS4, COX10, COX6B1, COX6A1, COX5A, COA6*, and *PPA1*, were also significantly correlated with poorer outcome.

CPT1A protein expression is a marker of poor prognosis

The correlation of CPT1A expression and poor prognosis was verified by IHC staining (Figure 4B). The N-MCL2/3 samples used for GEX (n=70) and IHC (n=45) analyses were overlapping by 23 patients, for which CPT1A gene and protein expression correlated (R=0.76; P=2.5x10^{-5}; *data not shown)*. Univariate Cox regression using CPT1A protein expression as a continuous value showed signifi-

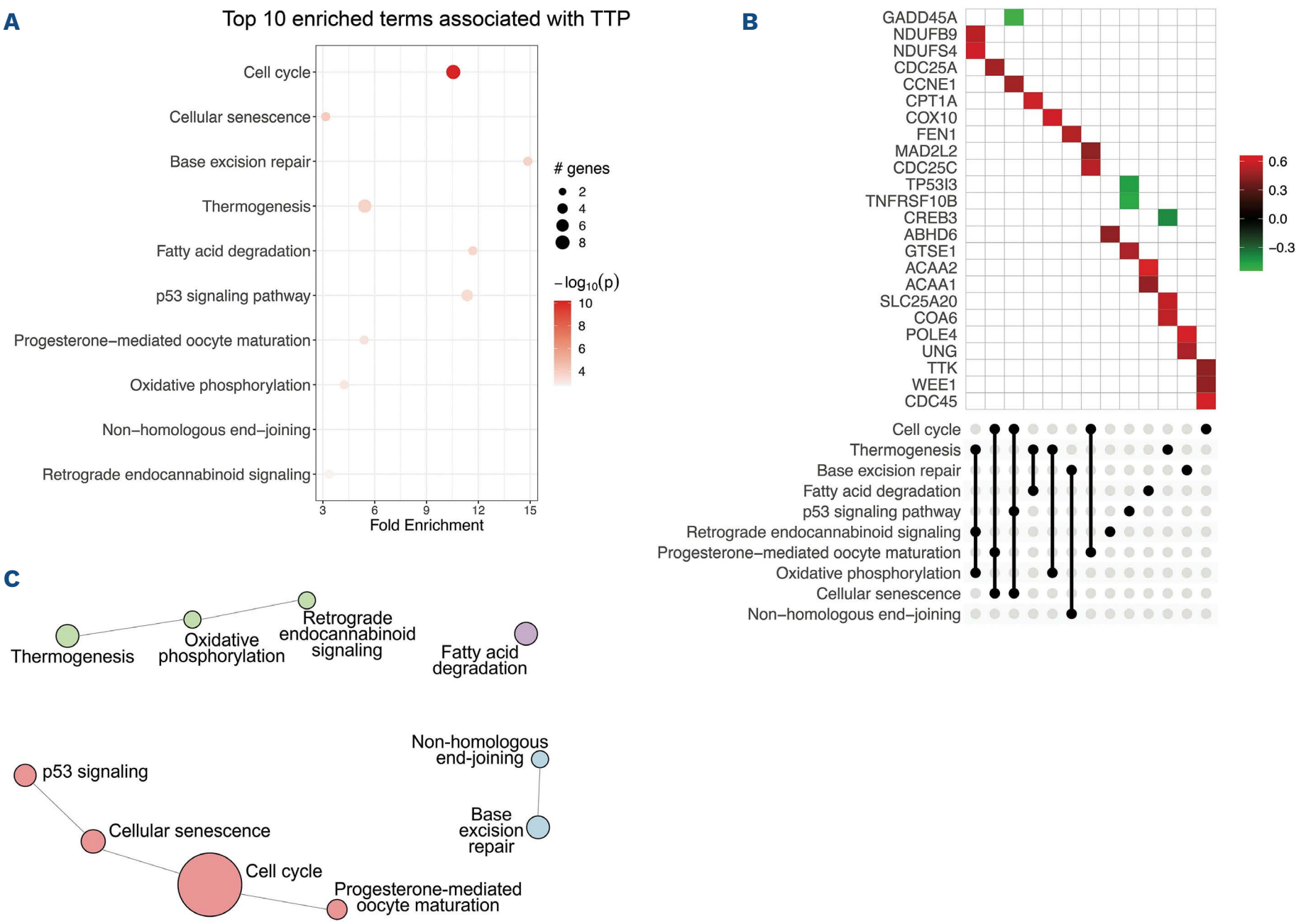

Figure 2. Pathways and associated genes related to inferior time to progression in mantle cell lymphoma. Top 10 enriched pathways associated with time to progression (TTP). Analysis was based on input of genes with log rank test $P<0.01$ as determined by cox regression using TTP as continuous variables. Bubble chart (A) x-axis displays enrichment based on cox regression β-values and bubble size corresponds to the number of input genes in the given pathway. UpSet plot (B) displaying genes within the top 10 enriched pathways with red denoting positive β-values (increased hazard) and green negative β-values (decreased hazard) in relation to survival. Pathway clustering based on overlapping genes (C). Circle size correspond to number of significant genes, color correspond to pathway cluster and distance between circles represent pathway relatedness based on overlapping genes.

cant association to inferior survival (hazard ratio [HR]=1.02; 95% confidence interval [CI]: 1.01-1.04) at 1% increase of CPT1A for both TTP and OS in N-MCL2/3 (Table 2). The association of CPT1A and inferior OS was validated in the BLISS cohort (n=129) (HR=1.01; 95% CI: 1.004–1.02). Data on TTP was lacking in the BLISS cohort, and thus no validation of response to treatment could be performed. At the univariate gene level, HR for *CPT1A* was 1.81 (95% CI: 1.29-2.54) and 1.64 (95% CI: 1.13-2.37) for TTP and OS, respectively. In order to define thresholds of CPT1A expression for patient stratification into low- and high-risk, optimal cut-offs of 15% for TTP and 69% for OS, were identified in N-MCL2/3. (Figure 5A, B, respectively). Applying the 15% cut-off defined for TTP to OS data separated the patients into groups with different outcome, but the log-rank test was not statistically significant (*Online Supplementary Figure S1)*. The HR for patients with high CPT1A was 3.36 (95% CI: 1.47–7.68) for TTP and 8.12 (95% CI: 2.75–23.9) for OS. The 69% cut-off for OS was validated in the BLISS cohort, where a significant association to survival was confirmed (HR=2.16; 95% CI: 1.33-3.51) (Figure 5C), while data for TTP was not available for BLISS. The higher HR for patients treated with the N-MCL2/3 protocol was expected, as the BLISS cohort had significantly higher median age and frequency of established risk factors, and heterogeneously treated patients. The association between CPT1A and inferior survival was independent of MIPI, morphology, proliferation (Table 2), and *TP53* (*Online Supplementary Table S1*) for TTP in N-MCL2/3. For OS, it was independent of morphology in BLISS, but not in N-MCL2/3. High CPT1A expression was significantly associated with high Ki-67 and non-classic morphology in both

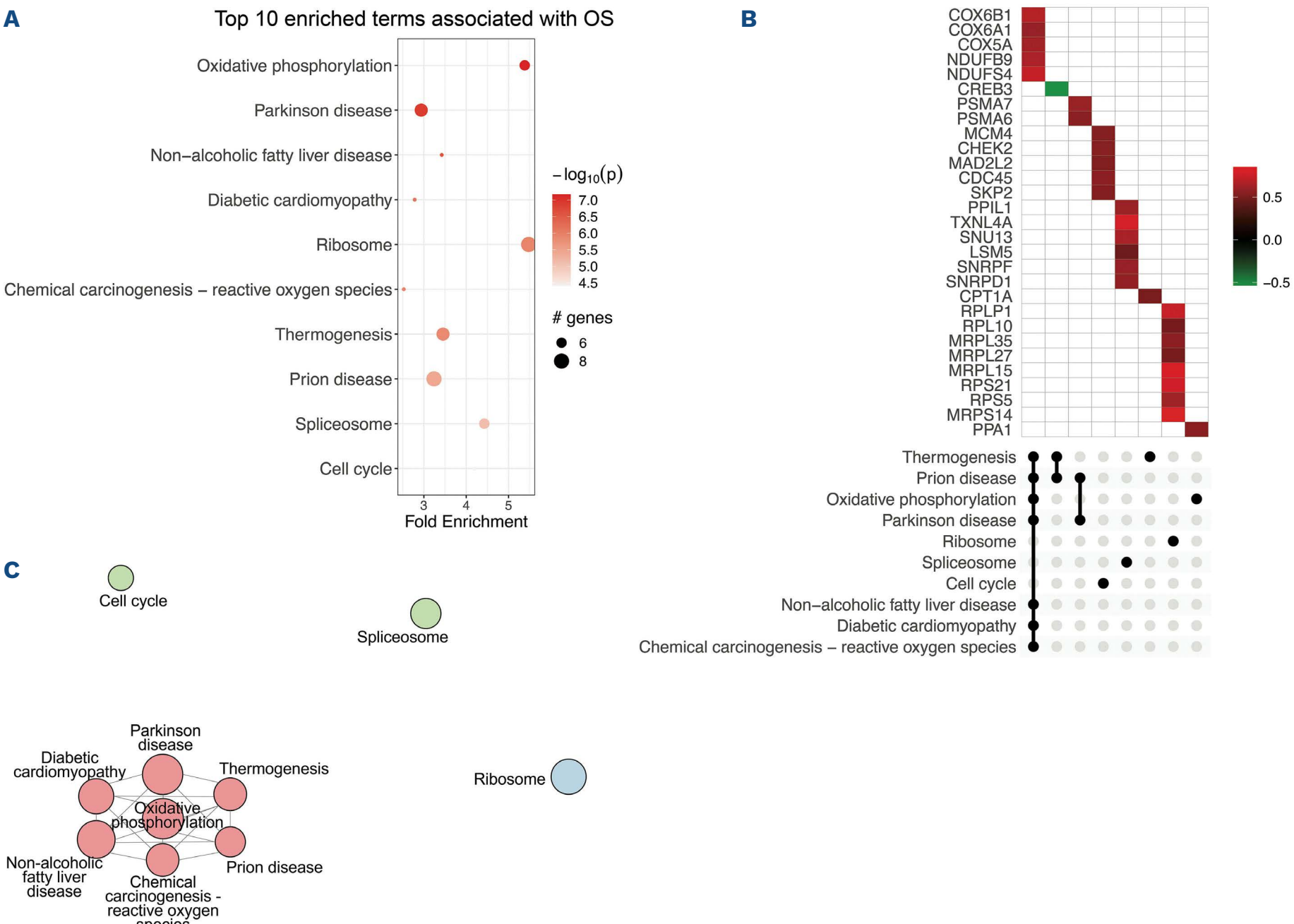

Figure 3. Pathways and associated genes related to inferior overall survival in mantle cell lymphoma. Top 10 enriched pathways associated with overall survival (OS). Analysis was based on input of genes with log-rank test $P<0.01$ as determined by cox regression using OS as continuous variables. Bubble chart (A) x-axis displays enrichment based on cox regression β-values and bubble size corresponds to the number of input genes in the given pathway. UpSet plot (B) displaying genes within the top 10 enriched pathways with red denoting positive β-values (increased hazard) and green negative β-values (decreased hazard) in relation to survival. Pathway clustering based on overlapping genes (C). Circle size correspond to number of significant genes, color correspond to pathway cluster and distance between circles represent pathway relatedness based on overlapping genes.

cohorts, but not to SOX11 (*Online Supplementary Figure S2*). We suggest that the prognostic value of CPT1A in relation to TTP is the most clinically relevant, and that future studies should use the defined 15% cut-off to assess high and low risk of short TTP.

Cell cycle is the dominating pathway associated with established high-risk mantle cell lymphoma factors

In order to investigate mechanisms underpinning known clinicopathological risk factors for MCL, differential GEX analysis was performed for Ki-67 high (>30% Ki-67-positive cells) *versus* Ki-67 low, non-classic *versus* classic morphology, and *TP53*-mutated *versus* wt in N-MCL2/3 (Figure 6A). A marked discrimination of high- *versus* low-proliferation cases was observed (21% DEG), with a significant enrichment peak of low *P* values and strong bias of upregulated genes in the Ki-67-high group (*Online Supplementary Figure S3A*), concordant with the notion that proliferation heavily impacts transcriptomic analyses. The top DEG ($P<1.0x10^{-4}$) were associated with 38 enriched pathways, and genes included in the top 10 pathways were exclusively upregulated in Ki-67-high (Figure 6B). The most significant pathway clusters were related to cell cycle, homologous recombination, and DNA replication (Figure 6C), with a significant part of key cell cycle genes being highly upregulated in Ki-67-high cases (*Online Supplementary Figure S4*).

With partly overlapping sample groups, pathways activated in non-classic *versus* classic morphology were also largely similar to those identified for high proliferation (Figure 6D, E). Compared to differential Ki-67, analysis based on morphology yielded weaker discrimination be-

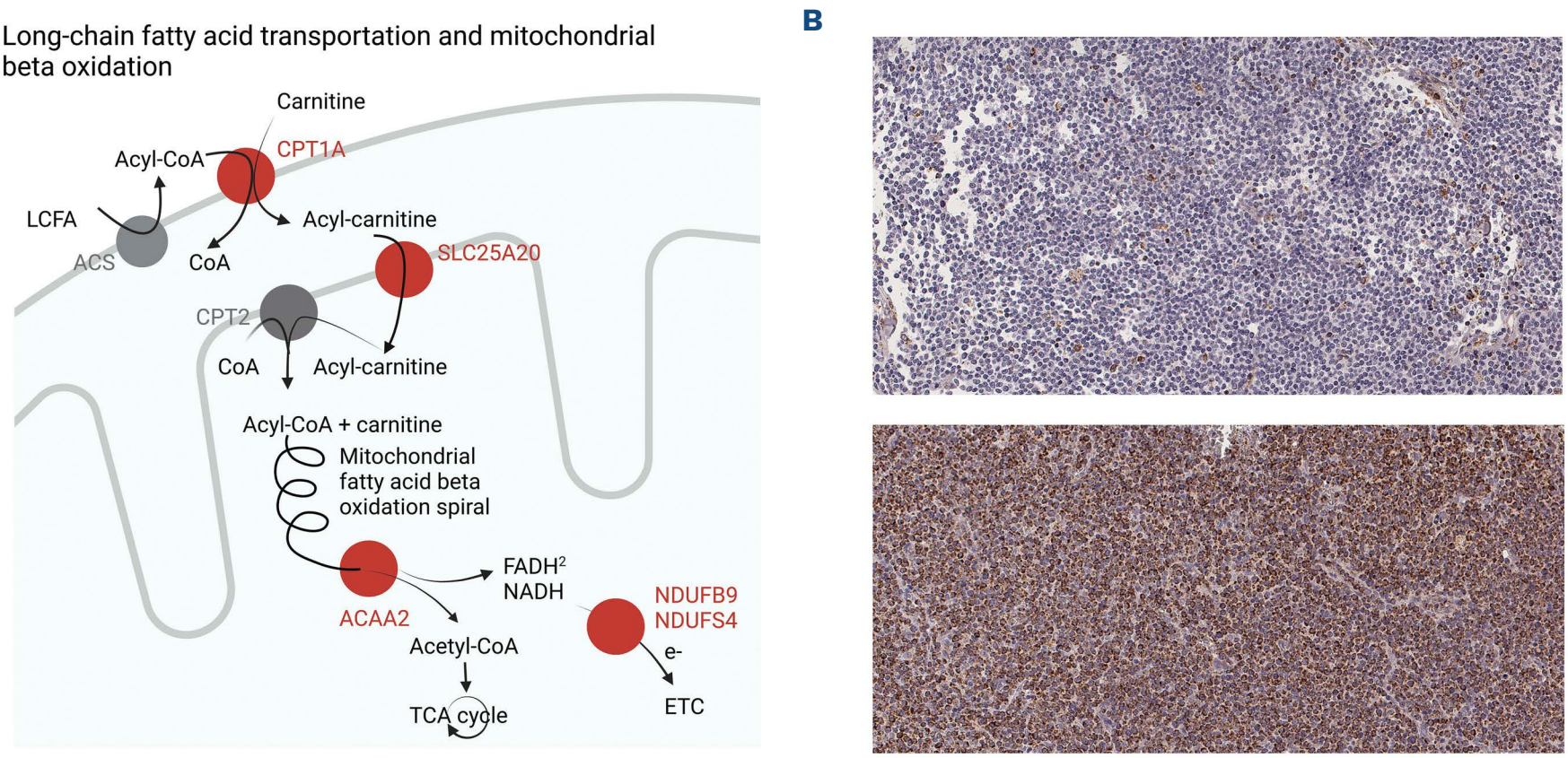

Figure 4. CPT1A expression, fatty acid transportation and mitochondrial fatty acid oxidation was associated with poor mantle cell lymphoma prognosis. (A) Active mitochondrial genes and pathways associated to shorter survival in the current cohort. Proteins marked in red represent some of the transcripts found to be upregulated in patients with poor outcome. LCFA: long-chain fatty acid; ACS: acetyl-CoA synthetase; TCA: tricarboxylic acid; ETC: electron transportation chain. (B) Representative high (94.5% positive cells) and low CPT1A (1.3% positive cells) immunohistochemistry staining.

tween groups, with 4.5% DEG (*Online Supplementary Figure S3B*). The top DEG (P<0.01) corresponded to 25 enriched pathways, again with dominating clusters of cell cycle, DNA repair and replication (Figure 6E). Genes that were specifically deregulated in non-classic *versus* classic morphology, and not significantly associated with the other risk factors included *MAP3K8*, *MAP2K6*, and *CXCL5*, involved in TNF signaling and related pathways.

FEN1 and WEE1 protein expression is associated with high-risk mantle cell lymphoma

Potentially targetable biomarkers were identified among upregulated genes in the high-risk MCL groups. *FEN1* and *WEE1* were found within the top deregulated pathways of Ki-67 high (Figure 5B) and non-classic morphology (Figure 6D) and were significantly associated with shorter TTP (Figure 2B). *FEN1* encodes a key enzyme involved in DNA repair[20,21] and *WEE1*, a kinase and key regulator of cell cycle through inhibition of Cdk1.[22] IHC validated the association to Ki-67 high and non-classic morphology for both WEE1 (*Online Supplementary Figure S5A, B*) and FEN1 (*Online Supplementary Figure S5D, E*). While dichotomized FEN1 expression was significantly correlated to OS (P<0.001) using a cut-off of 39% (*Online Supplementary Figure S5F*), no association to OS was seen for WEE1 on either gene (Figure 3B) or protein (*Online Supplementary Figure S5C*) level.

Transcriptional differences related to genetic alterations in MCL

Most genetic alterations in MCL are not associated with outcome, as for example *ATM*[4,23]. However, *TP53* mutations are present in 15% of tumors,[10,15] and define a highly aggressive sub-group of patients with poor response to currently available treatment regimens.[10] As *ATM* and *TP53* mutations were mutually exclusive in the patients included in the current study, we took the opportunity to investigate whether the transcriptional programs were distinct. The results are summarized in the *Online Supplementary Figures S6* and *S3C*. Despite the strong impact on outcome, a low proportion (2.1%) of DEG was found in *TP53*-mutated *versus* wt samples (*Online Supplementary Figure S3C*) while *ATM* aberrations were associated with deregulation of 10.7% of transcripts. Of interest, while *TP53* expression was indicated to be lower in *TP53*-mutated *versus* wt (P=0.18) samples, it was significantly higher in *ATM*-mutated *versus* wt (P=0.002) samples. When comparing *TP53*-mutated *versus* wt samples, the individual cell cycle pathway only appeared as the 16th most significant pathway (P=0.04), indicating that proliferation is not the sole dominating driver of *TP53*-mutated cases. In *ATM*-mutated cases, the most significantly enriched pathway was steroid biosynthesis (P=8x10^{-10}), but a network of pathways partly related to *TP53* was also found to be enriched (*Online Supplementary Figure S6D*) together with genes

Table 2. Univariate and multivariate Cox regression for CPT1A protein expression in both cohorts.

Type of analysis	Variable	Sub-group	HR (95% CI)	Outcome	N
N-MCL2/3					
Univariate	CPT1A continuous		1.02 (1.01-1.03)**	TTP	45
Univariate	CPT1A continuous		1.02 (1.01-1.04)***	OS	45
Univariate	CPT1A	≥5%[1]	3.36 (1.47-7.68)**	TTP	45
Univariate	CPT1A	≥69%[1]	8.12 (2.75-23.93)***	OS	45
Multivariate	CTP1A	≥15%[1]	3.11 (1.15-8.42)*	TTP	41
	MIPI	Intermediate[2]	1.25 (0.41-3.85)		
		High[2]	6.72 (2.08-21.76)**		
	Morphology	Blastoid/pleomorphic	2.13 (0.52-8.74)		
	Ki-67	≥30%	1.08 (0.33-3.48)		
Multivariate	CTP1A	≥69%[1]	6.18 (0.78-48.65)	OS	41
	MIPI	Intermediate[2]	2.01 (0.52-7.69)		
		High[2]	4.68 (0.98-22.39)		
	Morphology	Blastoid/pleomorphic	8.22 (1.59-42.36)*		
	Ki-67	≥30%	0.47 (0.08-2.74)		
BLISS					
Univariate	CPT1A continuous		1.01 (1.004-1.02)**	OS	129
Univariate	CPT1A	≥ 69%[1]	2.16 (1.33-3.51)**	OS	129
Multivariate	CTP1A	≥ 69%[1]	1.79 (1.07-2.99)*	OS	122
	Morphology	Blastoid/pleomorphic	0.66 (0.28-1.55)		
	Ki-67	≥ 30%	2.58 (1.3-5.13)		

[1]Maximally selected rank statistics cut-off values. [2]Mantle cell lymphoma International Prognostic Index (MIPI) low risk was used as reference category. *P<0.05; **P<0.01; ***P<0.001. CI: confidence interval; HR: hazard ratio; N: number of patients in the specific analyses; OS: overall survival; TTP: time to progression; N-MCL2/3: Nordic MCL group clinical trials 2 and 3; BLISS: biobank of lymphomas in Southern Sweden.

involved in apoptosis (*Online Supplementary Figure S6E*). The association of *ATM* mutations with tumor suppression and apoptosis provides a plausible explanation as to why *ATM* mutations do not confer a worse prognosis in MCL.

Discussion

More versatile treatment in combination with companion diagnostic strategies is needed to improve outcome for MCL patients. It has been proposed that MIPI,[7] which is nowadays used for prognostication but not stratification, could be used as a treatment selection tool if combined with assessment of proliferation and *TP53*-mutational status. This would improve the possibility to identify patients in need of alternative non-chemotherapy-based treatment. However, such a combined index considers only a narrow range of risk factors, not including intrinsic transcriptional differences in, for example, BCL2[24] or extrinsic factors such as variation in angiogenesis[25] or immune composition.[26,27] Deepened biological understanding of factors that influence early progression and relapse in patients treated with the current gold standard high-dose chemotherapy, would enable a more accurate treatment stratification and identification of novel targets for high-risk patients. To our knowledge, no/few studies have used outcome as a starting point to identify transcriptional profiles of MCL. Thus, to broaden the scope beyond established risk factors, we performed GEX analyses to decipher molecular mechanisms associated with outcome using a homogenously treated cohort of patients. For comparison and improved biological understanding of established risk factors, pathways and genes associated with *TP53* and *ATM* mutations, proliferation and non-classic morphology were also identified and described.

It is well known that the outcome of combinatorial treatment with immunochemotherapy, including rituximab, high-dose cytarabine and ASCT is related to several factors, including resistance to rituximab and/or cytarabine. Resistance to cytarabine has been extensively studied and involves the key rate-limiting step of the conversion of

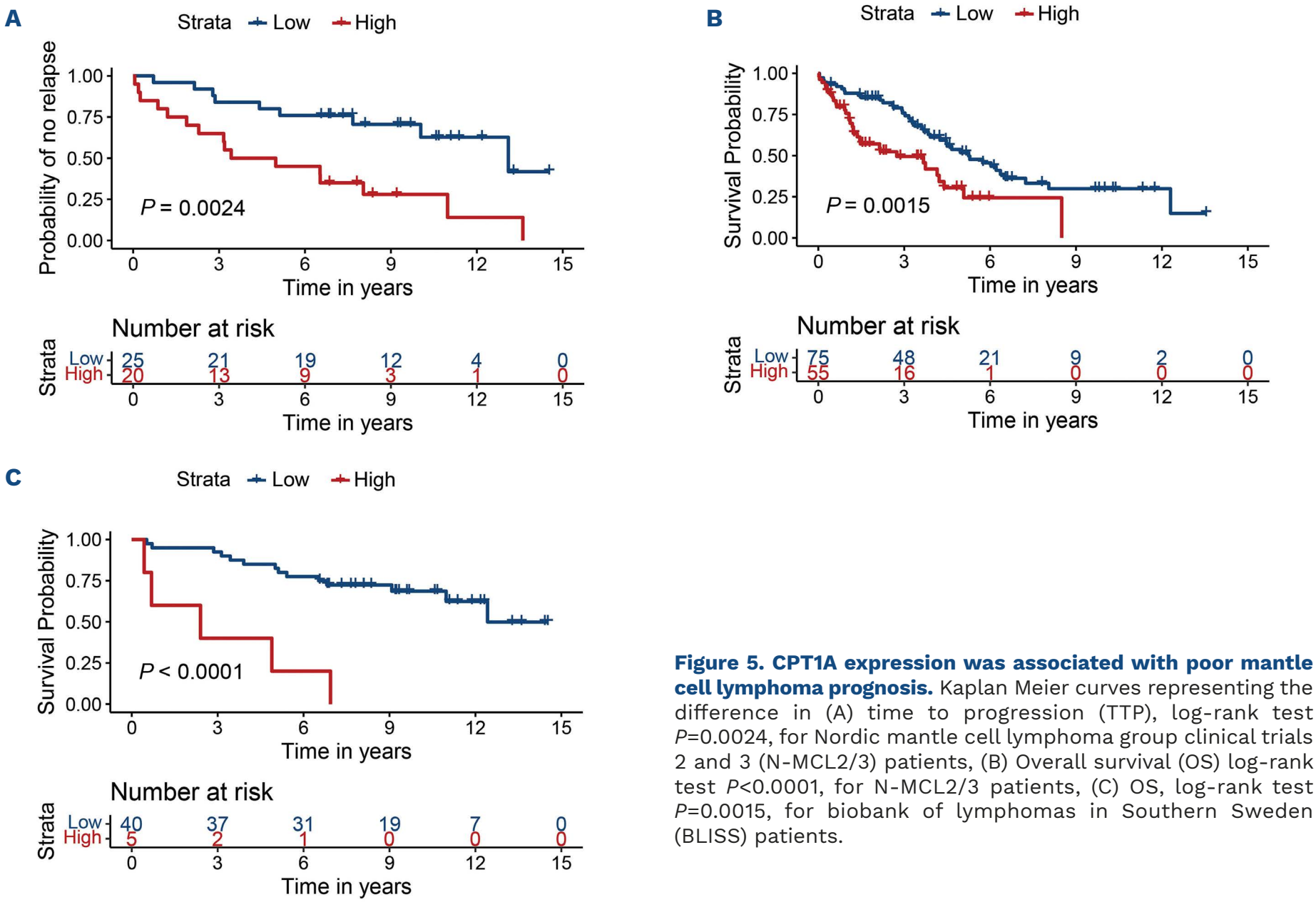

Figure 5. CPT1A expression was associated with poor mantle cell lymphoma prognosis. Kaplan Meier curves representing the difference in (A) time to progression (TTP), log-rank test *P*=0.0024, for Nordic mantle cell lymphoma group clinical trials 2 and 3 (N-MCL2/3) patients, (B) Overall survival (OS) log-rank test *P*<0.0001, for N-MCL2/3 patients, (C) OS, log-rank test *P*=0.0015, for biobank of lymphomas in Southern Sweden (BLISS) patients.

Ara-C to the active substance Ara-CTP.[28] We have previously shown that downregulation of deoxycytidine kinase (dCK) is a fundamental step during development of resistance, but no predictive markers are available. In line with previous observations, poor outcome was associated with key pathways associated with p53 regulation and proliferation. However, less-described pathways in MCL, including metabolic pathways such as thermogenesis, fatty acid degradation and oxidative phosphorylation, were also activated in patients with poor outcome. Of major interest, *CPT1A* and *SLC25A20*/CACT are both involved in the carnitine cycle,[29] with CPT1A being the rate-limiting step for mitochondrial oxidation of long-chain fatty acids and thus a key protein for fatty acid metabolism. In order to explore the applicability of CPT1A as a biomarker, we validated the overexpression and association to outcome using IHC and digital scoring. Also on the protein level, CPT1A as a continuous variable was a marker of poor prognosis, as measured by both TTP and OS. Importantly, CPT1A showed prognostic significance for TTP independent of MIPI and established risk factors, including *TP53*-mutational status, in multivariate analyses. Among the outcome variables, TTP is the most relevant prognostic measurement for treatment stratification, and the cut-off identified at 15% CPT1A-positive cells, should be the focus for future validation studies. This cut-off was also applied to OS data and was close to significant in the N-MCL2/3 cohort. No validation cohort with TTP data was available; however, the optimal cut-off value for OS at 69% CPT1A-positive cells was validated in the independent population-based BLISS cohort and was shown to be independent of proliferation and morphology.

The *CPT1* gene is situated on the q-arm of chromosome 11 and CPT1A is the most expressed isoform. The gene is regulated through a plethora of mechanisms including hormones, NF-Y and Sp proteins,[30] and microRNA.[31] CPT1A is well known to be expressed in cancer and associated to treatment resistance and aggressiveness of disease. In breast cancer, CPT1A is regulated by c-MYC or AMPK, and promotes metastasis or therapeutic resistance through several oncogenic signaling pathways.[32] Furthermore, it has been shown that BCL2 and CPT1A can interact on the surface of the mitochondria and regulate apoptosis in leukemia, and may thus antagonize apoptosis of BCL2-targeting agents.[33] When treating MCL patients with Bruton´s tyrosine kinase inhibitor Ibrutinib, enhanced

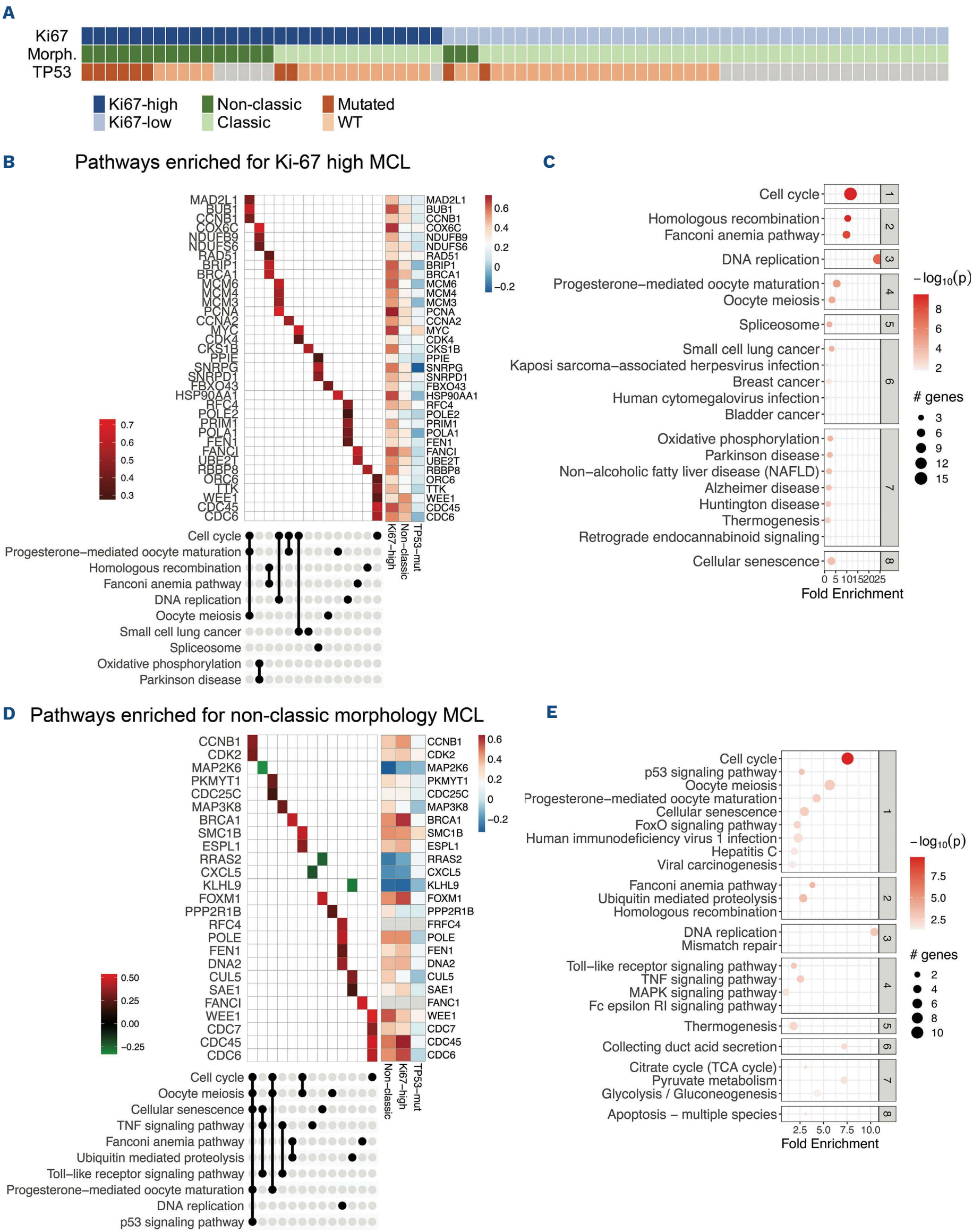

Continued on following page.

Figure 6. Genes associated with clinicopathological risk factors of mantle cell lymphoma. (A) Distribution of clinicopathological risk factors assessed, with 1 patient per column. Grey cells denote unknown *TP53*-mutational status. (B) Top 10 significantly ($P<1.4x10^{-4}$) enriched pathways associated with Ki-67 high mantle cell lymphoma (MCL) clustered by involvement of differentially expressed genes in an UpSet plot, colored by relative expression (all upregulated in Ki-67-high). Log fold-change (FC) values for Ki-67-high *vs.* -low, with non-classic *vs.* classic morphology (Morph.), and *TP53*-mutated *vs.* wild-type (wt) is shown for comparison. (C) Top 8 clusters of enriched pathways for Ki-67 high MCL. (D) Top 10 significantly ($P<2.1x10^{-3}$) enriched pathways associated with non-classic MCL clustered by involvement of differentially expressed genes in an UpSet plot, colored by relative expression with red and green denoting up- and downregulation in non-classic *vs.* classic MCL, respectively. Log FC values for non-classic *vs.* classic, with Ki-67-high *vs.* -low, and *TP53*-mutated *vs.* wt added for comparison. (E) Top 8 clusters of enriched pathways for non-classic MCL.

oxidative phosphorylation is associated with poor clinical outcome.[34] The activity of CPT1A inhibition in lymphomas is unknown, but *in vitro* evaluation of CPT1A inhibitors has shown high efficacy in several cancers such as high-grade serous ovarian cancer[35] and hepatocellular carcinoma,[36] and ability to sensitize cells to radiation in nasopharyngeal carcinoma.[37] In addition, we found eight other markers of active oxidative phosphorylation upregulated including *PPA1*, supporting previous observations that enhanced oxidative phosphorylation is associated with treatment resistance in MCL[34] and may be considered a potential target. Thus, the prognostic role associated to various treatments, including radiation in other types of cancers, indicates that CPT1A might be applicable for treatment stratification beyond the MCL2/3 regimen, although this remains to be determined.

Multiple efforts have been made to define the MCL transcriptome associated to key features such as proliferation,[38] the constitutive activation of NFκB and overexpression of *CCND1*.[39] As transcription-wide analyses are less suitable for clinical implementation, proliferation-associated signatures have been further developed into protein-based panels[40] and a 35-gene nanostring-based mRNA assay (MCL35).[41] It is evident, also from the current study, that proliferation is the factor associated with the largest transcriptional changes. Patients with non-classic morphology were highly overlapping with high proliferative cases, thus showing large commonality in pathways and genes that were deregulated. As expected, these pathways were mainly related to cell cycle and DNA repair. We identified *FEN1* and *WEE1* as associated to inferior TTP, as part of DNA repair and cell cycle pathways, respectively. FEN1 protein was significantly higher in Ki-67 high and non-classic morphology samples, and significantly associated with OS. *FEN1/RAD27*, encodes Flap endonuclease 1, which has been suggested as a promising target for patients with defects in homologous recombination, such as *BRCA1/BRCA2*-mutated tumors.[42] WEE1 protein was also confirmed to be associated with high proliferation and non-classic morphology, but no association to OS was seen on gene or protein level. *WEE1* is a key cell cycle regulator and the *in vitro* activity and synergistic effect of WEE1 and Chk1 inhibition has been demonstrated in MCL.[43] However, targeting single proliferation-associated genes has not been successful due to the many compensatory mechanisms.[44]

For long it was assumed that the overexpression of CCND1 mainly mediated increased proliferation of MCL cells. Today, it is more clear that it may also affect DNA repair, as shown in many cancers[45] including MCL.[46] Of interest, *ATM*, the most frequent (>40%) genetic aberration in MCL, affects DNA repair,[3] but does not confer a survival disadvantage. While *ATM* mutations are common, *TP53* mutations are the dominating molecular indicator of poor prognosis in MCL.[3] As it has been shown by us[4] and others[23] that co-occurrence of *TP53* and *ATM* mutations are infrequent in MCL, we set out to investigate if they share common molecular pathways. Pathways associated with *ATM* mutations were distinct from *TP53*-mutated MCL and dominated by the steroid biosynthesis pathway. Of interest, individuals with germline mutations in the *ATM* gene are known to have increased plasma cholesterol and triglyceride levels, and *ATM* has been demonstrated to facilitate clearance of apolipoproteins in plasma.[49] Thus, *ATM* mutations may contribute to altered lipid metabolism and steroid biosynthesis.

Today, proposed strategies for prediction of response to treatment in MCL are focused on MIPI in combination with assessment of proliferation and *TP53* mutational status. In this comprehensive overview of the transcriptional landscape in MCL, we have explored high-risk features of MCL beyond these established factors. We show that fatty acid metabolism is deregulated in MCL and, thus propose that complementary investigations of metabolism may contribute to defining high-risk MCL through routine assessment of CPT1A.

Disclosures

CWE is currently employed by Genmab. MJ has received research support from Abbvie, AstraZeneca, Janssen, Gilead, BMS and Roche; and honoraria from Abbvie, AstraZeneca, BMS, Genmab, Janssen, Novartis, Incyte, EUSApharma, Gilead, and Roche. All other authors have no conflicts of interest to disclose.

Contributions

ASG performed data and statistical analysis and wrote the manuscript; JMR took part in the study plan, performed

data analysis and took part in the writing of the manuscript; CWE, SH, KG, RR, AK, CG and MJ were involved in the collection of the material and/or clinical data; AP took part in the pathology review; SE planned the study, interpreted results, and assisted in writing the manuscript. All authors approved the final version of the manuscript.

Acknowledgments

The authors would like to thank the Nordic lymphoma group, and specifically the Nordic MCL network; Lina Olsson and May Hassan at the SpatialOmics@LU core facility at the Department of Immunotechnology, Lund University for assisting with expression analysis; Björn Nodin at the Department of Clinical Studies, Lund University for assisting with tissue cuts and IHC.

Funding

This project has received funding from the European Union's Horizon 2020 research and innovation programme under the Marie Skłodowska-Curie grant agreement N 754299, Cancerfonden (2016/465, 19 0309Pj and 21 1561 Pj), Mats Paulssons Stiftelse för forskning, innovation och samhällsbyggande, Stiftelsen Stefan Paulssons cancerfond, and CREATE Health. All financial support was granted to SE.

Data-sharing statement

Original data and protocols are available upon reasonable request.

References

1. Grimm KE, O'Malley DP. Aggressive B cell lymphomas in the 2017 revised WHO classification of tumors of hematopoietic and lymphoid tissues. Ann Diagn Pathol. 2019;38:6-10.
2. Jain P, Wang M. Mantle cell lymphoma: 2019 update on the diagnosis, pathogenesis, prognostication, and management. Am J Hematol. 2019;94(6):710-725.
3. Hill HA, Qi X, Jain P, et al. Genetic mutations and features of mantle cell lymphoma: a systematic review and meta-analysis. Blood Adv. 2020;4(13):2927-2938.
4. Rodrigues JM, Porwit A, Hassan M, Ek S, Jerkeman M. Targeted genomic investigations in a population-based cohort of mantle cell lymphoma reveal novel clinically relevant targets. Leuk Lymphoma. 2021;62(11):2637-2647.
5. Rule S, Dreyling M, Goy A, et al. Ibrutinib for the treatment of relapsed/refractory mantle cell lymphoma: extended 3.5-year follow up from a pooled analysis. Haematologica. 2019;104(5):e211-e214.
6. Pu JJ, Savani M, Huang N, Epner EM. Mantle cell lymphoma management trends and novel agents: where are we going? Ther Adv Hematol. 2022;13:20406207221080743.
7. Silkenstedt E, Linton K, Dreyling M. Mantle cell lymphoma - advances in molecular biology, prognostication and treatment approaches. Br J Haematol. 2021;195(2):162-173.
8. Kolstad A, Laurell A, Jerkeman M, et al. Nordic MCL3 study: 90Y-ibritumomab-tiuxetan added to BEAM/C in non-CR patients before transplant in mantle cell lymphoma. Blood. 2014;123(19):2953-2959.
9. Geisler CH, Kolstad A, Laurell A, et al. Long-term progression-free survival of mantle cell lymphoma after intensive front-line immunochemotherapy with in vivo-purged stem cell rescue: a nonrandomized phase 2 multicenter study by the Nordic Lymphoma Group. Blood. 2008;112(7):2687-2693.
10. Eskelund CW, Dahl C, Hansen JW, et al. TP53 mutations identify younger mantle cell lymphoma patients who do not benefit from intensive chemoimmunotherapy. Blood. 2017;130(17):1903-1910.
11. Klaus B, Reisenauer S. An end to end workflow for differential gene expression using Affymetrix microarrays. F1000Res. 2016;5:1384.
12. Ulgen E, Ozisik O, Sezerman OU. pathfindR: an R package for comprehensive identification of enriched pathways in Omics data through active subnetworks. Front Genet. 2019;10:858.
13. Kononen J, Bubendorf L, Kallioniemi A, et al. Tissue microarrays for high-throughput molecular profiling of tumor specimens. Nat Med. 1998;4(7):844-847.
14. Hothorn T, Lausen B. On the exact distribution of maximally selected rank statistics. Computational Statistics & Data Analysis. 2003;43(2):121-137.
15. Rodrigues JM, Hassan M, Freiburghaus C, et al. p53 is associated with high-risk and pinpoints TP53 missense mutations in mantle cell lymphoma. Br J Haematol. 2020;191(5):796-805.
16. Hoster E, Dreyling M, Klapper W, et al. A new prognostic index (MIPI) for patients with advanced-stage mantle cell lymphoma. Blood. 2008;111(2):558-565.
17. Hoster E, Rosenwald A, Berger F, et al. Prognostic value of Ki-67 index, cytology, and growth pattern in mantle-cell lymphoma: results from randomized trials of the European Mantle Cell Lymphoma Network. J Clin Oncol. 2016;34(12):1386-1394.
18. Hoster E, Klapper W, Hermine O, et al. Confirmation of the mantle-cell lymphoma International Prognostic Index in randomized trials of the European Mantle-Cell Lymphoma Network. J Clin Oncol. 2014;32(13):1338-1346.
19. Hoster E. Prognostic relevance of clinical risk factors in mantle cell lymphoma. Semin Hematol. 2011;48(3):185-188.
20. Klungland A, Lindahl T. Second pathway for completion of human DNA base excision-repair: reconstitution with purified proteins and requirement for DNase IV (FEN1). EMBO J. 1997;16(11):3341-3348.
21. Querol-Audi J, Yan C, Xu X, et al. Repair complexes of FEN1 endonuclease, DNA, and Rad9-Hus1-Rad1 are distinguished from their PCNA counterparts by functionally important stability. Proc Natl Acad Sci U S A. 2012;109(22):8528-8533.
22. Harvey SL, Charlet A, Haas W, Gygi SP, Kellogg DR. Cdk1-dependent regulation of the mitotic inhibitor Wee1. Cell. 2005;122(3):407-420.
23. Mareckova A, Malcikova J, Tom N, et al. ATM and TP53 mutations show mutual exclusivity but distinct clinical impact in mantle cell lymphoma patients. Leuk Lymphoma. 2019;60(6):1420-1428.
24. Montraveta A, Xargay-Torrent S, Rosich L, et al. Bcl-2 high mantle cell lymphoma cells are sensitized to acadesine with

ABT-199. Oncotarget. 2015;6(25):21159-21172.
25. Annese T, Ingravallo G, Tamma R, et al. Inflammatory infiltrate and angiogenesis in mantle cell lymphoma. Transl Oncol. 2020;13(3):100744.
26 Balsas P, Veloza L, Clot G, et al. SOX11, CD70, and Treg cells configure the tumor-immune microenvironment of aggressive mantle cell lymphoma. Blood. 2021;138(22):2202-2215.
27. Rodrigues JM, Nikkarinen A, Hollander P, et al. Infiltration of CD163-, PD-L1- and FoxP3-positive cells adversely affects outcome in patients with mantle cell lymphoma independent of established risk factors. Br J Haematol. 2021;193(3):520-531.
28. Di Francia R, Crisci S, De Monaco A, et al. Response and toxicity to cytarabine therapy in leukemia and lymphoma: from dose puzzle to pharmacogenomic biomarkers. Cancers (Basel). 2021;13(5):966.
29. Ramsay RR, Gandour RD, van der Leij FR. Molecular enzymology of carnitine transfer and transport. Biochim Biophys Acta. 2001;1546(1):21-43.
30. Steffen ML, Harrison WR, Elder FF, Cook GA, Park EA. Expression of the rat liver carnitine palmitoyltransferase I (CPT-Ialpha) gene is regulated by Sp1 and nuclear factor Y: chromosomal localization and promoter characterization. Biochem J. 1999;340(Pt 2)(Pt 2):425-432.
31. Schlaepfer IR, Joshi M. CPT1A-mediated fat oxidation, mechanisms, and therapeutic potential. Endocrinology. 2020;161(2):bqz046.
32. Tan Z, Zou Y, Zhu M, et al. Carnitine palmitoyl transferase 1A is a novel diagnostic and predictive biomarker for breast cancer. BMC Cancer. 2021;21(1):409.
33. Paumen MB, Ishida Y, Han H, et al. Direct interaction of the mitochondrial membrane protein carnitine palmitoyltransferase I with Bcl-2. Biochem Biophys Res Commun. 1997;231(3):523-525.
34. Zhang L, Yao Y, Zhang S, et al. Metabolic reprogramming toward oxidative phosphorylation identifies a therapeutic target for mantle cell lymphoma. Sci Transl Med. 2019;11(491):eaau1167.
35. Huang D, Chowdhury S, Wang H, et al. Multiomic analysis identifies CPT1A as a potential therapeutic target in platinum-refractory, high-grade serous ovarian cancer. Cell Rep Med. 2021;2(12):100471.
36. Ren M, Xu H, Xia H, Tang Q, Bi F. Simultaneously targeting SOAT1 and CPT1A ameliorates hepatocellular carcinoma by disrupting lipid homeostasis. Cell Death Discov. 2021;7(1):125.
37. Tan Z, Xiao L, Tang M, et al. Targeting CPT1A-mediated fatty acid oxidation sensitizes nasopharyngeal carcinoma to radiation therapy. Theranostics. 2018;8(9):2329-2347.
38. Demajo S, Albero R, Clot G, et al. A Cyclin D1-dependent transcriptional program predicts clinical outcome in mantle cell lymphoma. Clin Cancer Res. 2021;27(1):213-225.
39. Balaji S, Ahmed M, Lorence E, Yan F, Nomie K, Wang M. NF-kappaB signaling and its relevance to the treatment of mantle cell lymphoma. J Hematol Oncol. 2018;11(1):83.
40. Hartmann E, Fernandez V, Moreno V, et al. Five-gene model to predict survival in mantle-cell lymphoma using frozen or formalin-fixed, paraffin-embedded tissue. J Clin Oncol. 2008;26(30):4966-4972.
41. Scott DW, Abrisqueta P, Wright GW, et al. New molecular assay for the proliferation signature in mantle cell lymphoma applicable to formalin-fixed paraffin-embedded biopsies. J Clin Oncol. 2017;35(15):1668-1677.
42. Guo E, Ishii Y, Mueller J, et al. FEN1 endonuclease as a therapeutic target for human cancers with defects in homologous recombination. Proc Natl Acad Sci U S A. 2020;117(32):19415-19424.
43. Chila R, Basana A, Lupi M, et al. Combined inhibition of Chk1 and Wee1 as a new therapeutic strategy for mantle cell lymphoma. Oncotarget. 2015;6(5):3394-3408.
44. Tchakarska G, Le Lan-Leguen A, Roth L, Sola B. The targeting of the sole cyclin D1 is not adequate for mantle cell lymphoma and myeloma therapies. Haematologica. 2009;94(12):1781-1782.
45. Jirawatnotai S, Hu Y, Michowski W, et al. A function for cyclin D1 in DNA repair uncovered by protein interactome analyses in human cancers. Nature. 2011;474(7350):230-234.
46. Mohanty S, Mohanty A, Sandoval N, et al. Cyclin D1 depletion induces DNA damage in mantle cell lymphoma lines. Leuk Lymphoma. 2017;58(3):676-688.
47. Bellanger S, de Gramont A, Sobczak-Thepot J. Cyclin B2 suppresses mitotic failure and DNA re-replication in human somatic cells knocked down for both cyclins B1 and B2. Oncogene. 2007;26(51):7175-7184.
48. Liu Q, Li A, Tian Y, et al. The CXCL8-CXCR1/2 pathways in cancer. Cytokine Growth Factor Rev. 2016;31:61-71.
49. Wu J, Xiao Y, Liu J, et al. Potential role of ATM in hepatocyte endocytosis of ApoE-deficient, ApoB48-containing lipoprotein in ApoE-deficient mice. Int J Mol Med. 2014;33(2):462-468.